Studies on Phosphatidylserine by Tandem Quadrupole and Multiple Stage Quadrupole Ion-Trap Mass Spectrometry with Electrospray Ionization: Structural Characterization and the Fragmentation Processes

Fong-Fu Hsu and John Turk

Mass Spectrometry Resource, Division of Endocrinology, Diabetes, Metabolism, and Lipid Research, Department of Internal Medicine, Washington University School of Medicine, St. Louis, Missouri, USA

Low-energy CAD product-ion spectra of various molecular species of phosphatidylserine (PS) in the forms of $[M - H]^-$ and $[M - 2H + Alk]^-$ in the negative-ion mode, as well as in the forms of $[M + H]^+$, $[M + Alk]^+$, $[M - H + 2Alk]^+$, and $[M - 2H + 3Alk]^+$ (where Alk = Li, Na) in the positive-ion mode contain rich fragment ions that are applicable for structural determination. Following CAD, the $[M - H]^-$ ion of PS undergoes dissociation to eliminate the serine moiety (loss of $C_3H_5NO_2$) to give a $[M - H - 87]^-$ ion, which equals to the $[M - H]^-$ ion of a phoshatidic acid (PA) and give rise to a MS^3-spectrum that is identical to the MS^2-spectrum of PA. The major fragmentation process for the $[M - 2H + Alk]^-$ ion of PS arises from primary loss of 87 to give rise to a $[M - 2H + Alk - 87]^-$ ion, followed by loss of fatty acid substituents as acids (R_xCO_2H, x = 1,2) or as alkali salts (e.g., R_xCO_2Li, x = 1,2). These fragmentations result in a greater abundance of $[M - 2H + Alk - 87 - R_2CO_2H]^-$ than $[M - 2H + Alk - 87 - R_1CO_2H]^-$ and a greater abundance of $[M - 2H + Alk - 87 - R_2CO_2Li]^-$ than $[M - 2H + Alk - 87 - R_1CO_2Li]^-$; while further dissociation of the $[M - 2H + Alk - 87 - R_{2(or\ 1)}CO_2Li]^-$ ions gives a preferential formation of the carboxylate anion at *sn*-1 ($R_1CO_2^-$) over that at *sn*-2 ($R_2CO_2^-$). Other major fragmentation process arises from differential loss of the fatty acid substituents as ketenes (loss of $R_x'CH{=}CO$, x = 1,2). This results in a more prominent $[M - 2H + Alk - R_2'CH{=}CO]^-$ ion than $[M - 2H + Alk - R_1'CH{=}CO]^-$ ion. Ions informative for structural characterization of PS are of low abundance in the MS^2-spectra of both the $[M + H]^+$ and the $[M + Alk]^+$ ions, but are abundant in the MS^3-spectra. The MS^2-spectrum of the $[M + Alk]^+$ ion contains a unique ion corresponding to internal loss of a phosphate group probably via the fragmentation processes involving rearrangement steps. The $[M - H + 2Alk]^+$ ion of PS yields a major $[M - H + 2Alk - 87]^+$ ion, which is equivalent to an alkali adduct ion of a monoalkali salt of PA and gives rise to a greater abundance of $[M - H + 2Alk - 87 - R_1CO_2H]^+$ than $[M - H + 2Alk - 87 - R_2CO_2H]^+$. Similarly, the $[M - 2H + 3Alk]^+$ ion of PS also yields a prominent $[M - 2H + 3Alk - 87]^+$ ion, which undergoes consecutive dissociation processes that involve differential losses of the two fatty acyl substituents. Because all of the above tandem mass spectra contain several sets of ion pairs involving differential losses of the fatty acid substituents as ketenes or as free fatty acids, the identities of the fatty acyl substituents and their positions on the glycerol backbone can be easily assigned by the drastic differences in the abundances of the ions in each pair. (J Am Soc Mass Spectrom 2005, 16, 1510–1522) © 2005 American Society for Mass Spectrometry

Phosphatidylserine (PS, 1,2-diacyl-*sn*-glycero-3-phosphorylserine) occurs quite widely in nature but usually in low concentrations (3–10%) of the total phospholipids. The compound was first isolated by Folch from brain [1] and the exact structure was later established by Baer and Maurukas [2, 3].

In yeast and prokaryotes, PS is made by a PS synthase that uses CDP-diacylglycerol and serine [4]. However, in mammals, PS is generated by a base-exchange reaction in which L-serine substitutes the choline and ethanolamine moieties of phosphatidylcholine and phosphatidylethanolamine, respectively, with the participation of PS synthase 1 and PS synthase 2, respectively, to yield PS and choline or ethanolamine [5]. The major route for PE synthesis in

Published online July 15, 2005

Address reprint requests to Dr. F.-F. Hsu, Department of Internal Medicine, Washington University School of Medicine, 660 S. Euclid, Box 8127, St. Louis, MO 63110, USA. E-mail: fhsu@im.wustl.edu

1044-0305/05/$30.00
doi:10.1016/j.jasms.2005.04.018

Received October 22, 2004
Revised April 28, 2005
Accepted April 29, 2005

cells is from the mitochondrial decarboxylation of PS using decarboxylase [6].

In addition to its presumed contribution to membrane structure, PS has been evidenced to engage in a number of key cellular processes. For example, PS is an activator of several enzymes such as protein kinase C [7], Na^+/K^+ ATPase [8], and neutral sphingomyelinase [9, 10]. The externalization of PS on the cell surface is thought to be a critical signal for platelet activation during the blood clotting cascade [11], for skeletal muscle development [12], and for macrophage recognition of cells undergoing apoptosis [13–18]. Phosphatidylserine receptor is recognized to be essential for removing apoptotic cells during mammalian development of lung and brain [19].

Mass spectrometric methods with FAB ionization toward to the structural characterization of PS in the $[M + H]^+$ form have been previously performed by tandem sector [20] and tandem quadrupole mass spectrometers [21] following collisionally activated dissociation (CAD). More structural information can be obtained from low-energy CAD of the $[M - H]^-$ species in the negative-ion mode [21]. Although brief studies on the adduct ions in the fashions of $[M - H + Co]^+$ and of $[M - H + Ni]^+$ using ion-trap mass spectrometers have been reported [22], there have been very few detailed studies of the molecular ion species generated by electrospray ionization (ESI) [23]. Herein, we describe ESI with tandem quadrupole and with quadrupole ion-trap mass spectrometric methods to characterize PS in the forms of $[M - H]^-$ and $[M - 2H + Alk]^-$ in the negative-ion mode, as well as in the forms of $[M + Alk]^+$, $[M - H + 2Alk]^+$ and $[M - 2H + 3Alk]^+$ (Alk = Li, Na) in the positive-ion mode. The fragmentation processes under low-energy CAD are also proposed.

Materials and Methods

Phosphatidylserine and phosphatidic acid standards (sodium salt) were purchased from Avanti Polar lipid (Alabaster, AL). All solvents are of research grade and were purchased from Fisher Scientific (Pittsburgh, PA). To convert sodium into lithium salt form, PS (in Na^+ form) in chloroform was added to distilled water, sonicated for 2 min. The mixture was centrifuged for 5 min at 3000 rpm. Lower phase containing PS was collected, diluted with methanol, and LiOH (0.1 umol/uL in methanol) was added. The final solution contains 1 nmol/uL LiOH and 10–100 pmol/uL PS in methanol/chloroform (vol/vol, 2/1). Deuterium labeled 16:0/18:1-PS were prepared by dissolving d_0-16:0/18:1-PS standard in 95/5 (vol/vol) CH_3OD/CH_3OH. When being subjected to ESI, the solution gives the $[M - H]^-$ ions at *m/z* 760 (d_0-16:0/18:1-PS), 761 (d_1-16:0/18:1-PS), 762 (d_2-16:0/18:1-PS), and 763 (d_3-16:0/18:1-PS) ions in a ratio of 0.25/0.8/1/0.35.

Mass Spectrometry

Low-energy CAD tandem mass spectrometry experiments were conducted on a Finnigan (San Jose, CA) TSQ 7000 mass spectrometer equipped with ICIS data system or on a LCQ DECA ion-trap mass spectrometer with X-calibur operation system. Solutions containing PS were continuously infused into the ESI source with a syringe pump at a flow rate of 1 uL/min. The skimmer was at ground potential and the electrospray needle was set at 4.5 kV. The temperature of the heated capillary was 260 °C. For product-ion spectra obtained with a triple stage quadrupole (TSQ) instrument, the precursor ions were selected in the first quadrupole (Q1), collided with Ar (2.3 mTorr) in the rf-only second quadrupole (Q2) using a collision energy of 30–35 eV, and analyzed in the third quadrupole (Q3). Both Q1 and Q3 were tuned to unit mass resolution and scanned at a rate of 3 s/scan. The mass spectra were accumulated in the profile mode, typically for 5 min for a tandem mass spectrum. For CAD tandem mass spectra obtained with a quadrupole ion-trap mass spectrometer (ITMS), the automatic gain control of the ion trap was set to 5×10^7, with a maximum injection time of 400 ms. Helium was used as the buffer and collision gas at a pressure of 1×10^{-3} mbar. The mass resolution was 0.6 Da at half peak height. To maximize the sensitivity and to obtain a more even distribution of the fragment ions for the MS^n spectra ($n \geq 2$), a relative collision energy varied from 30 to 38% was used with an activation time at 100 ms, and the activation q value at 0.25.

Results and Discussion

When being subjected to ESI in the negative-ion mode, phosphatidylserine yields a prominent $[M - H]^-$ ion. In the presence of alkali ion, however, molecular species in the form of $[M - 2H + Alk]^-$ (Alk = Li, Na) can also be observed, attributable to the fact that PS possesses two anionic charge sites of which one can attach to an Alk^+. In the positive-ion mode, PS yields $[M + H]^+$ ion, and adduct ions in the fashions of $[M + Alk]^+$, $[M - H + 2Alk]^+$, and $[M - 2H + 3Alk]^+$ (Alk = Li, Na) can also be formed, when being ionized in the presence of alkali metal ion. However, the sensitivity in the positive-ion mode is about one order of magnitude less than that observed as the $[M - H]^-$ ion in the negative-ion mode. Structural characterization of the various molecular species of PS by tandem quadrupole and ion-trap mass spectrometry and the fragmentation pathways leading to ion formations are described below.

The $[M - H]^-$ Ions

PS produces a prominent $[M - H]^-$ ion by ESI along with $[M - H - 87]^-$ ion, indicating that PS is labile and readily undergoes in-source fragmentation to expel the serine head group (loss of $C_3H_5NO_2$, 87 Da). This is consistent with the notion that the IT MS^2-spectrum of

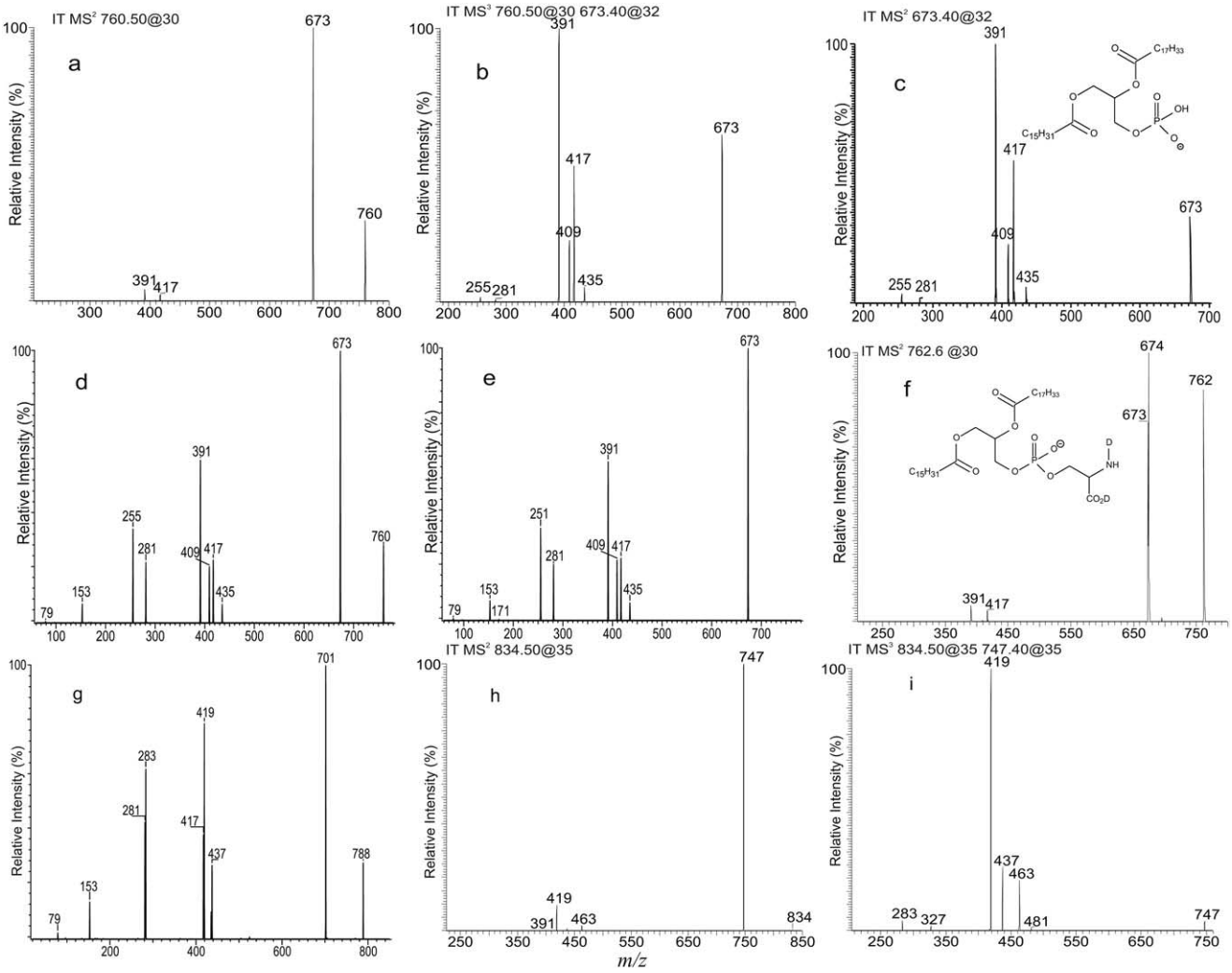

Figure 1. (**a**) The IT MS^2-spectrum of the $[M - H]^-$ ion of 16:0/18:1-PS at *m/z* 760, (**b**) its IT MS^3-spectrum of the *m/z* 673 ion ($[M - H - 87]^-$) (760 → 673), (**c**) the IT MS^2-spectrum of the $[M - H]^-$ ion of 16:0/18:1-PA at *m/z* 673, (**d**) the tandem quadrupole product-ion spectrum of the $[M - H]^-$ ion of 16:0/18:1-PS at *m/z* 760, (**e**) the source CAD product-ion-spectrum of the *m/z* 673 ion (760 → 673), (**f**) the IT MS^2-spectrum of the $[M - H]^-$ ion of d_2-16:0/18:1-PS at *m/z* 762, (**g**) the tandem quadrupole product-ion spectrum of the $[M - H]^-$ ion of 18:0/18:1-PS at *m/z* 788, (**h**) the IT MS^2-spectrum of the $[M - H]^-$ ion of 18:0/22:6-PS at *m/z* 834, and (**i**) its IT MS^3-spectrum of *m/z* 747 (834 → 747).

the $[M - H]^-$ ion of 1-palmitoyl-2-oleoyl-3-*sn*-glycero-phosphoserine (16:0/18:1-PS) at *m/z* 760 is dominated by the *m/z* 673 ion ($[M - H - 87]^-$) (Figure 1a), which is equivalent to the $[M - H]^-$ ion of 1-palmitoyl-2-oleoyl-3-*sn*-glycero-phosphatidic acid (16:0/18:1-PA) and gives rise to a MS^3-spectrum (760 → 673) (Figure 1b) identical to that arising from an authentic 16:0/18:1-PA standard (Figure 1c). The fragmentation process is also consistent with the findings that the tandem quadrupole product-ion spectrum of the $[M - H]^-$ ion at *m/z* 760 (Figure 1d) is nearly identical to that from the $[M - H]^-$ ion of standard 16:0/18:1-PA and that of the *m/z* 673 ion (760 → 673) (Figure 1e), generated by in-source CAD of 16:0/18:1-PS. The ions at *m/z* 391 ($[M - H]^- - 87 - R_2CO_2H$) and *m/z* 417 ($[M - H]^- - 87 - R_1CO_2H$) arising from the respective loss of the fatty acids at *sn*-1 and at *sn*-2 are, respectively, more abundant than the ions at *m/z* 409 ($[M - H]^- - 87 - R'_2CH{=}C{=}O$) and *m/z* 435 ($[M - H]^- - 87 - R'_1CH{=}C{=}O$), arising from their corresponding ketene losses (Figure 1a–e). These spectrum features are characteristic of PA [24] and further support the idea that the major ions observed in the tandem quadrupole product-ion spectra mainly arise from the consecutive dissociation of the $[M - H - 87]^-$ ion, rather than from direct dissociation of the $[M - H]^-$ ions via a concerted pathway [23].

The loss of the $C_3H_5NO_2$ moiety to yield the $[M - H - 87]^-$ ion may involve the participation of an exchangeable hydrogen that is attached to the amino group (Scheme 1, route *a*). This assumption is based on observation of both the *m/z* 673 and 674 ions in the IT MS^2-spectrum of d_2-16:0/18:1-PS at *m/z* 762 (Figure 1f) obtained by H—D exchange, which occurred probably at one of the two exchangeable hydrogens of the amino

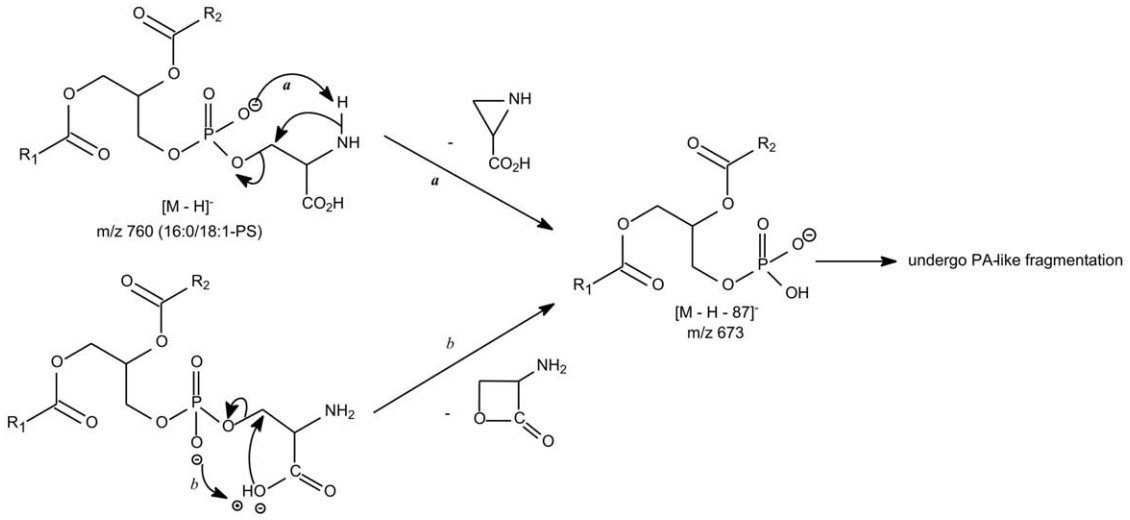

Scheme 1. The fragmentation processes proposed for the $[M - H]^-$ ion of PS.

group and at the acidic hydrogen attached to carboxylate group. The loss of the $C_3H_5NO_2$ moiety can also arise from the nucleophilic attack of the phosphate anionic site on the acidic hydrogen (Scheme 1, route *b*) [22, 23]. This fragmentation process is supported by observation of both *m/z* 673 and 674 ions (the abundance ratio is 5 to 4) in the IT MS^2-spectrum of d_1-16:0/18:1-PS at *m/z* 761 (data not shown), of which probably only the acidic hydrogen attached to the carboxylate group was replaced by a deuterium.

The *m/z* 391 ion ($[M - H - 87 - R_2CO_2H]^-$) is more abundant than the *m/z* 417 ($[M - H - 87 - R_1CO_2H]^-$) ion, and the *m/z* 409 ion ($[M - H - 87 - R'_2CH{=}C{=}O]^-$) is also more abundant than the *m/z* 435 ion ($[M - H - 87 - R'_1CH{=}C{=}O]^-$), consistent with the notion that the ion reflecting loss of the fatty acyl substituent as an acid or as a ketene at *sn*-2 is more abundant than that arising from the analogous loss at *sn*-1 [24, 25]. The $R_1CO_2^-$ ion at *m/z* 255 is also more abundant than the $R_2CO_2^-$ ion at *m/z* 281, a characteristic feature observed for PA [24]. The above results provide information to identify the fatty acyl substituents and their position in the glycerol backbone. The product-ion spectrum of the $[M - H]^-$ ion of 18:0/18:1-PS at *m/z* 788 (Figure 1g) is also similar to the product-ion spectrum of *m/z* 701 (788 → 701) generated by source CAD of *m/z* 788 (not shown). The primary loss of the $C_3H_5NO_2$ moiety to a PA-like precursor ion pathway for the $[M - H]^-$ ion of PS is also supported by the IT MS^2-spectrum of the $[M - H]^-$ ion of 18:0/22:6-PS at *m/z* 834 (Figure 1h), which contains a prominent ion at *m/z* 747, and by the IT MS^3-spectrum of *m/z* 747 (834 → 747) (Figure 1i), which is a typical IT MS^2-spectrum of 18:0/22:6-PA.

The $[M - 2H + Alk]^-$ Ions

In contrast, the product-ion spectra of the $[M - 2H + Li]^-$ ion of 16:0/18:1-PS at *m/z* 766 obtained with a TSQ (Figure 2a) and with an ITMS (Figure 2b) instruments contain major ions at *m/z* 528 and 502 arising from loss of the 16:0- and of the 18:1-fatty acyl substituents as ketenes, respectively, (Scheme 2, route *a*), and the ions at *m/z* 484 and 510 arising from the corresponding losses of the fatty acyl substituents as acids are of low abundance. The *m/z* 502 ion ($[M - 2H + Li - R'_2CH{=}CO]^-$) that reflects loss of the 18:1-fatty acyl ketene at *sn*-2 is more abundant than the *m/z* 528 ($[M - 2H + Li - R'_1CH{=}CO]^-$) ion, reflecting loss of the 16:0-fatty acyl ketene at *sn*-1. This feature is similar to that observed for the $[M - H]^-$ ion of phosphatidylethanolamines (PE), consistent with the suggestion that the gaseous $[M - H]^-$ ion of PE is basic and undergoes more favorable loss of the fatty acid substituent as a ketene than as an acid [25]. After the remaining proton on the $[M - H]^-$ ion of PS is replaced by an Li^+, the gaseous $[M - 2H + Li]^-$ ion may become more basic than the $[M - H]^-$ ion, and the gas-phase basicity is probably similar to that of the $[M - H]^-$ ion of PE. The ions at *m/z* 528 ($[M - 2H + Li - R'_1CHCO]^-$) and 502 ($[M - 2H + Li - R'_2CHCO]^-$) are equivalent to the $[M - 2H + Li]^-$ ions of 1- and 2-lysophosphatidylserine, respectively, and undergo further loss of the $C_3H_5NO_2$ moiety to yield ions at *m/z* 441 and 415, respectively, (Scheme 2, route a'_1). The ions at *m/z* 528 and 502 also give rise to *m/z* 417 and 391 by elimination of serine as a lithium salt (route a'_2).

The primary loss of the $C_3H_5NO_2$ moiety to a *m/z* 679 ion (766 − 87) (Scheme 2, route *b*), followed by loss of the 18:1-fatty acyl chain at *sn*-2 and loss of the 16:0-fatty acyl chain at *sn*-1 as lithium salts, respectively, gives rise to ions at *m/z* 391 ($679 - C_{17}H_{33}CO_2Li$) and 417 ($679 - C_{15}H_{31}CO_2Li$) (Scheme 2, route b'_1). Again, the *m/z* 391 ion is more abundant than the *m/z* 417 ion. The above results are consistent with the notion that ions reflecting the losses at *sn*-2 are more abundant than those reflecting the analogous losses at *sn*-1. The fragmentation processes are supported by the MS^3-spectra of *m/z* 679 (Figure 3c), *m/z* 528 (Figure 3d) and *m/z* 502 (not shown).

The $R_1CO_2^-$ ion at *m/z* 255 is more abundant than the $R_2CO_2^-$ ion at *m/z* 281, similar to that observed for PA but reversed to that observed for PE. This is attributable

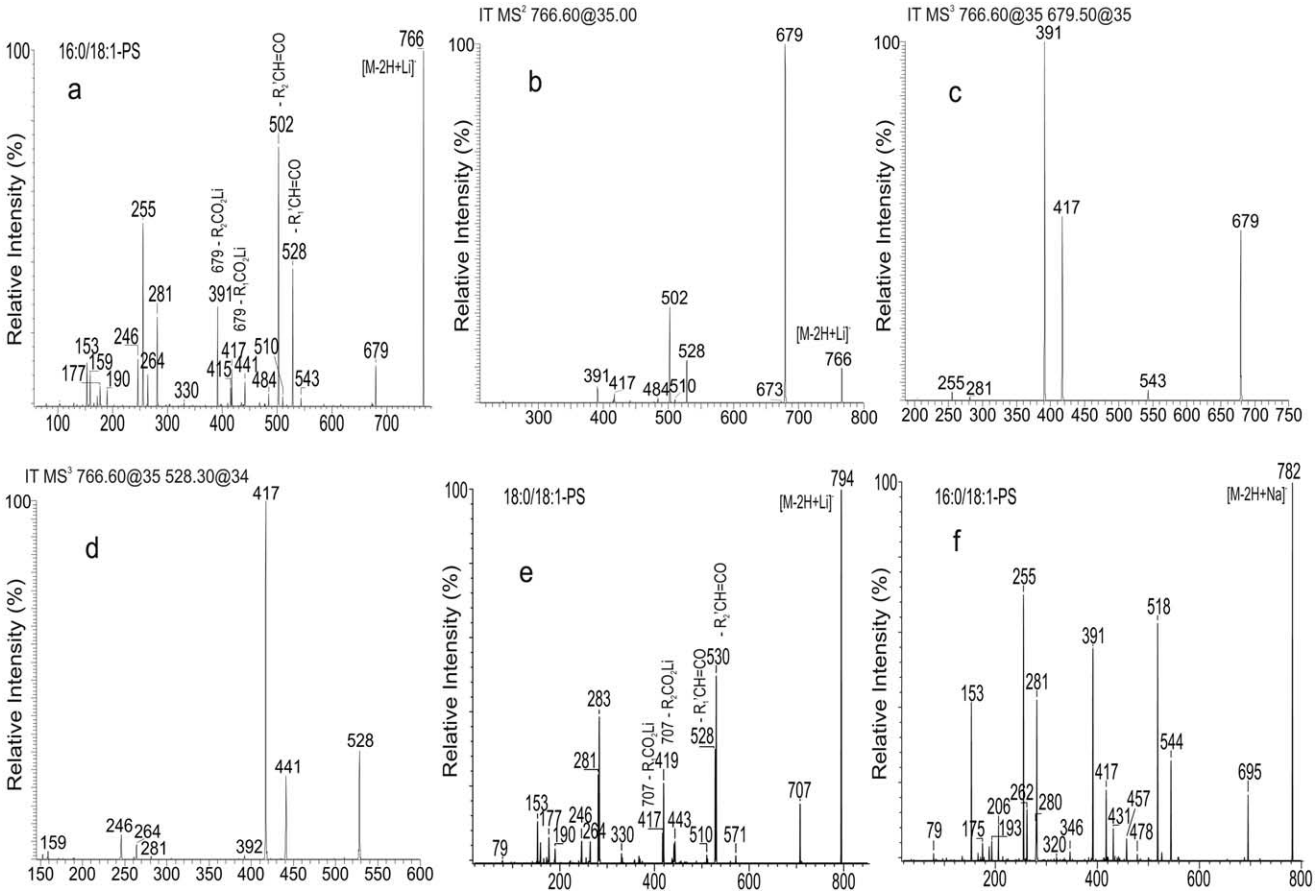

Figure 2. The product-ion spectra of the $[M - 2H + Li]^-$ ion of 16:0/18:1-PS at *m/z* 766 obtained with (**a**) a TSQ, and (**b**) an ITMS instruments. (**c**), (**d**) The IT MS^3-spectra of (**c**) the *m/z* 679 (766 → 679), and (**d**) the *m/z* 528 (766 → 528) ions arising from *m/z* 766. (**e**), (**f**) The product-ion spectra of (**e**) the $[M - 2H + Li]^-$ ion of 18:0/18:1-PS at *m/z* 794, and of (**f**) the $[M - 2H + Na]^-$ ion of 16:0/18:1-PS at *m/z* 782.

to the fact that the carboxylate anions at *m/z* 255 and 281 mainly arise from *m/z* 391 and 417, respectively, by loss of a stable dicylic glycerophosphate ester moiety of 136 (Scheme 2, route b''_1), as previously described for PA [24].

The combined losses of the fatty acyl substituent at *sn*-2 and at *sn*-1 as ketenes from *m/z* 766 yield the *m/z* 264 ion ($[M - H - R'_1CH{=}CO - R'_2CH{=}CO]^-$), which further dissociates to *m/z* 177 (264 − 87) by elimination of the $C_3H_5NO_2$ moiety, while the *m/z* 246 ion ($[M - H - R'_1CH{=}CO - R'_2CO_2H]^- + [M - H - R'_2CH{=}CO - R'_1CO_2H]^-$) arises from primary loss of a fatty acyl substituent as a ketene followed by loss of the remaining fatty acyl substituent as an acid. These fragmentation pathways are supported by observation of the ions at *m/z* 264 and 246 in the MS^3-spectrum of *m/z* 528 (Figure 2d). Ions characteristic to serine head group are observed at *m/z* 190, arising from cleavage of the C3—O bond (Scheme 2, route *c*), via the fragmentation process similar to that previously observed for PE [25]. The analogous ions from the fragmentation processes are also observed in the product-ion spectra of the $[M - 2H + Li]^-$ ions of 18:0/18:1-PS at *m/z* 784 (Figure 2e) and the $[M - 2H + Na]^-$ ion of the 16:0/18:1-PS at *m/z* 782 (Figure 2f).

The $[M + H]^+$ ions

Both the MS^2-spectra of the $[M + H]^+$ ion of 16:0/18:1-PS at *m/z* 762 obtained with a TSQ (Figure 3a) and with an ITMS (not shown) instruments are dominated by a $[M + H - 185]^+$ ion at *m/z* 577 (762 − 185) arising from loss of the phosphoserine moiety (Scheme 3), similar to that previously observed by FAB tandem mass spectrometry, and provides limited information for structural characterization [21]. Although the identities of the fatty acyl substituents can be recognized by the 16:0- and 18:1-acylium ions at *m/z* 239 and 265, respectively, as well as by the ions at *m/z* 339 and 313 arising from losses of the 16:0- and the 18:1-fatty acyl substituents as ketenes from *m/z* 577, respectively, these ions are of low abundance and lack the specificity for assignment of the position of the fatty acyl substituents on the glycerol backbone.

In contrast, the IT MS^3-spectrum of the *m/z* 577 (762 → 577) ion (Figure 3b) contains a prominent

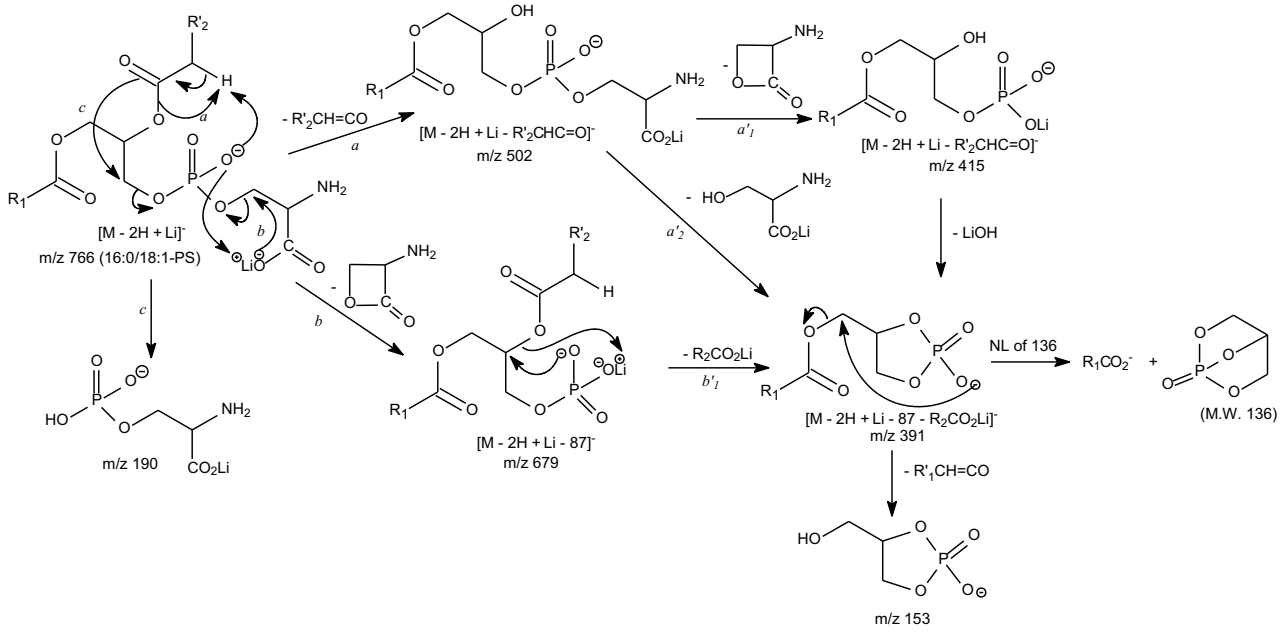

Scheme 2. The fragmentation processes proposed for the $[M - 2H + Li]^-$ ion of PS. Only the preferential pathways involving the participation of the fatty acid substituent at *sn*-2 are shown. The *m/z* values are those observed for 16:0/18:1-PS.

18:1-acylium ion at *m/z* 265, which is more abundant than the 16:0-acylium at *m/z* 239, along with ion at *m/z* 247 (265 − H_2O), which is also more abundant than the *m/z* 221 (239 − H_2O) ion. The spectrum also contains the *m/z* 321 ion (577 − R_1CO_2H) arising from further loss of the 16:1-fatty acid substituent at *sn*-1, whereas the analogous ion expected at *m/z* 295 arising from loss of the 18:1-fatty acid at *sn*-2 is not present. The drastic differences in the abundances of the above ion pairs resulting from differential losses of the fatty acyl substituents provide information for assignment of the positions of the fatty acyl moieties on the glycerol backbone. Similar results were also observed for the MS^3-spectrum of *m/z* 605 (790 → 605) (Figure 3c), arising from 18:0/18:1-PS at *m/z* 790. However, the IT MS^3-spectrum of the *m/z* 651 ion (836 → 651) (Figure 3d) arising from 18:0/22:6-PS at *m/z* 836 is dominated by ions at *m/z* 367 attributable to the loss of the 18:0-fatty acyl moiety at *sn*-1, and at *m/z* 341 due to loss of the 22:6-fatty acyl substituent as a ketene. The preferential loss of polyunsaturated fatty acid moiety as a ketene has been previously observed for PE and PC [26, 27].

The $[M + Alk]^+$ Ions

The use of alkali metal adduct ions, in particular the $[M + Li]^+$ ions, for structural characterization of various lipids by ESI coupled with tandem mass spectrometry has been very successful [26–29]. The MS^2-spectrum of the $[M + Li]^+$ ion of 16:0/18:1-PS at *m/z* 768 obtained with a TSQ instrument (Figure 4a) contains prominent ions at *m/z* 577, arising from loss of phosphoserine as a lithium salt and at *m/z* 192, corresponding to a lithiated phosphoserine ion, via cleavage of the C3—OP bond similar to that observed for the $[M + H]^+$ ion (Scheme 3). The ion at *m/z* 681 (768 − $C_3H_5NO_2$) is of low-abundance and gives rise to ions at *m/z* 425 (681 − R_1CO_2H) and 399 (681 − R_2CO_2H) by loss of the 16:0- and 18:1-fatty acid, respectively. The *m/z* 425 ion is more abundant than the *m/z* 399 ion, similar to that observed for the $[M + Li]^+$ ion of phosphatidylethanolamine [26], and provides information for assignment of the position of the fatty acyl substituents on the glycerol backbone. Similar results were also observed for the $[M + Li]^+$ ion of 18:0/18:1-PS at *m/z* 796 (Figure 4b).

The IT MS^2-spectrum of the $[M + Li]^+$ of 16:0/18:1-PS at *m/z* 768 (Figure 4c) contains ions similar to those observed in Figure 4a, but the ions at *m/z* 681 and 670 are among the most prominent. As shown in Figure 4d, the MS^3-spectrum of the *m/z* 681 ion (768 → 681) yields ions at *m/z* 583 and 577 arising from loss of the phosphoric acid group as an acid and as a lithium salt, respectively. The spectrum also contains ions at *m/z* 425 (681 − R_1CO_2H) and 399 (681 − R_2CO_2H) resulting from loss of the 16:0- and 18:1-fatty acid moiety, respectively, along with ions at *m/z* 443 (681 − $R'_1CH{=}CO$) and 417 (681 − $R'_2CH{=}CO$), arising from the corresponding losses as fatty acyl ketenes.

The prominence of the ion at *m/z* 670 in Figure 4c is of interest. The ion corresponds to loss of the phosphoric acid and its formation may involve a rearrangement process in which the anionic site of the serine head group renders nucleophilic attack on C-3 of the glycerol backbone, followed by expulsion of the phosphoric acid moiety to yield a lithiated triacyl glycerol-like ion at *m/z* 670 (Scheme 4). This fragmentation process is sup-

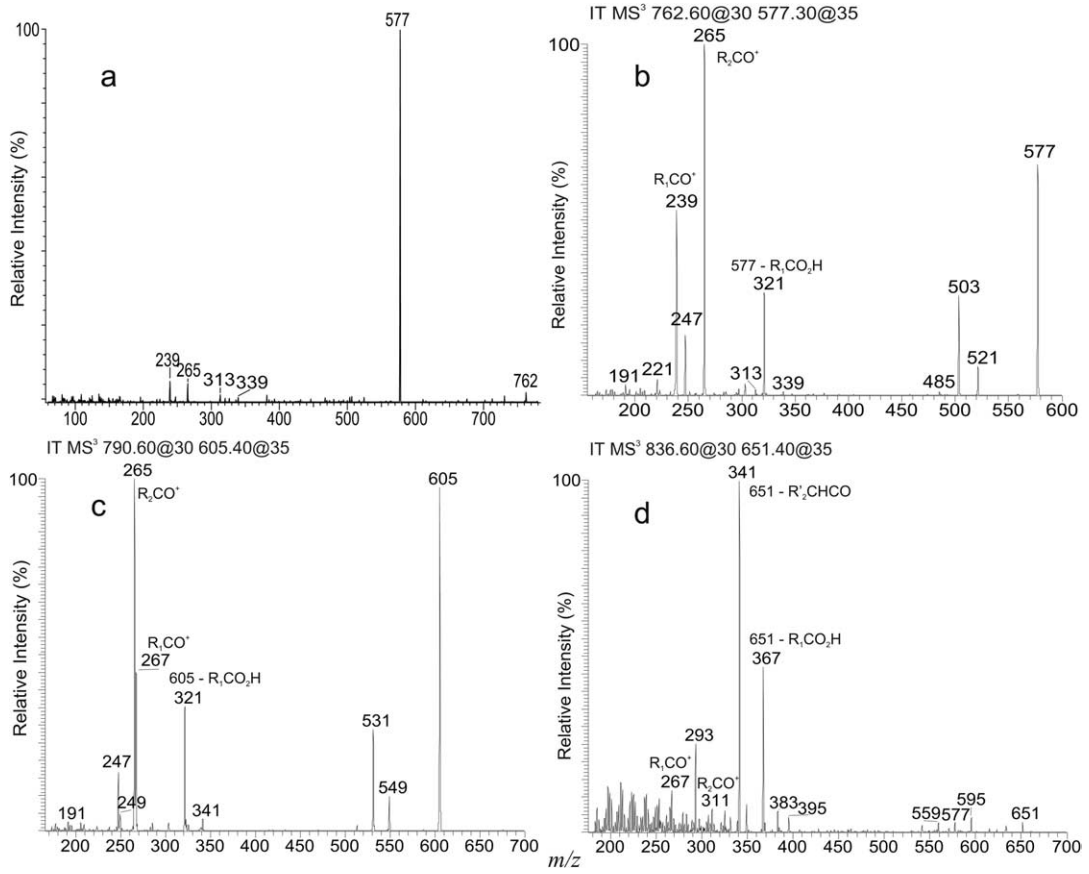

Figure 3. (**a**) The tandem quadrupole product-ion spectrum of the $[M + H]^+$ ion of 16:0/18:1-PS at *m/z* 762. (**b**)–(**d**) The IT MS^3-spectra of (**b**) the *m/z* 577 ion (762 → 577) arising from 16:0/18:1-PS, of (**c**) the *m/z* 605 ion (790 → 605) arising from 18:0/18:1-PS, and of (**d**) the *m/z* 651 ion (836 → 651) arising from 18:0/22:6-PS.

ported by the MS^3-spectrum of *m/z* 670 (Figure 4e), which contains ions at *m/z* 583 and 577, corresponding to loss of $C_3H_5NO_2$ and $C_3H_4NO_2Li$ (as a lithium salt) moieties (Scheme 4a, route *a*), respectively; and ions at *m/z* 414 (route *b*) and 388 resulting from the respective loss of the 16:0- and of the 18:1-fatty acid moieties. In contrast, the ion at *m/z* 670 is of low abundance in the product-ion spectrum obtained with a TSQ instrument (Figure 4a). This is consistent with the suggestion that elimination of the phosphate moiety involves a rear-

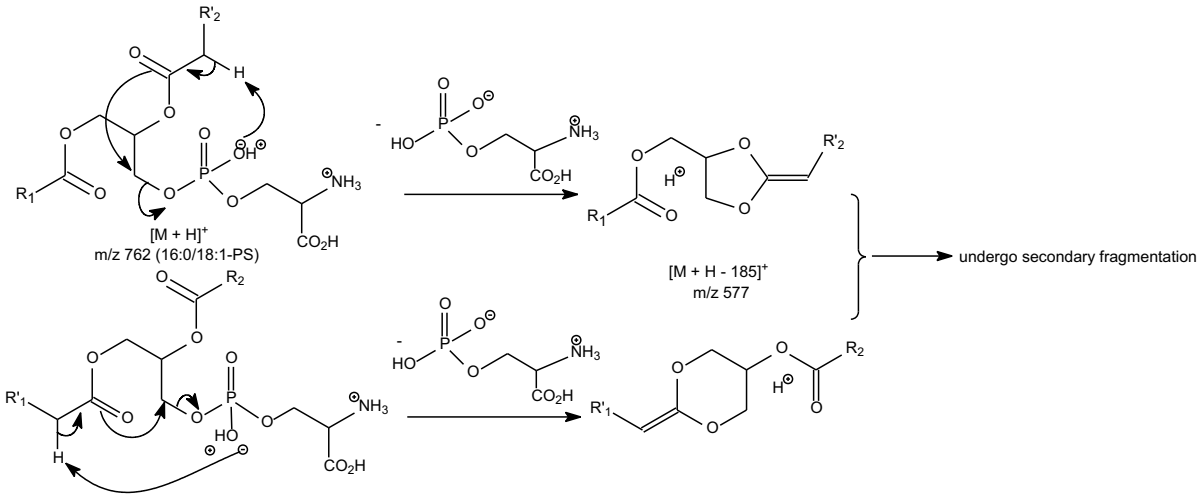

Scheme 3. The fragmentation processes proposed for the $[M + H]^+$ ion of 16:0/18:1-PS.

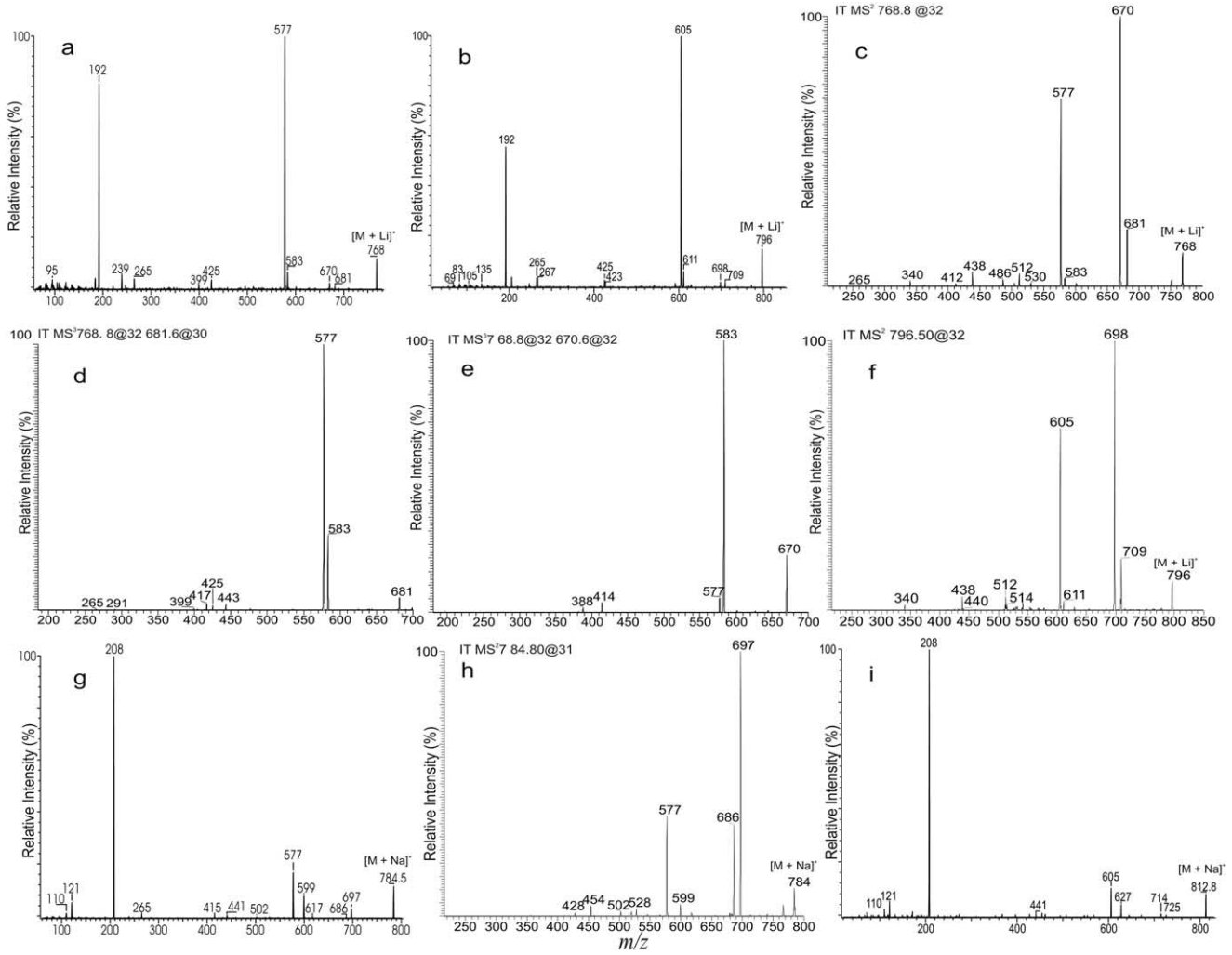

Figure 4. The tandem quadrupole product-ion spectra of the $[M + Li]^+$ ions of (**a**) 16:0/18:1-PS at *m/z* 768, and of (**b**) 18:0/18:1-PS at *m/z* 796. (**c**)–(**e**) The IT MS^2-spectra of the $[M + Li]^+$ ions of (**c**) 16:0/18:1-PS at *m/z* 768, and its IT MS^3-spectra of (**d**) *m/z* 681 ion (768 → 681), and (**e**) *m/z* 670 ion (768 → 670). (**f**) The IT MS^2-spectrum of the $[M + Li]^+$ ion of 18:0/18:1-PS at *m/z* 796. (**g**)–(**i**) The product-ion spectra of the $[M + Na]^+$ ions of 16:0/18:1-PS at *m/z* 784 obtained with (**g**) a TSQ instrument, (**h**) an ITMS instrument, and (**i**) of 18:0/18:1-PS at *m/z* 812 obtained with a TSQ instrument.

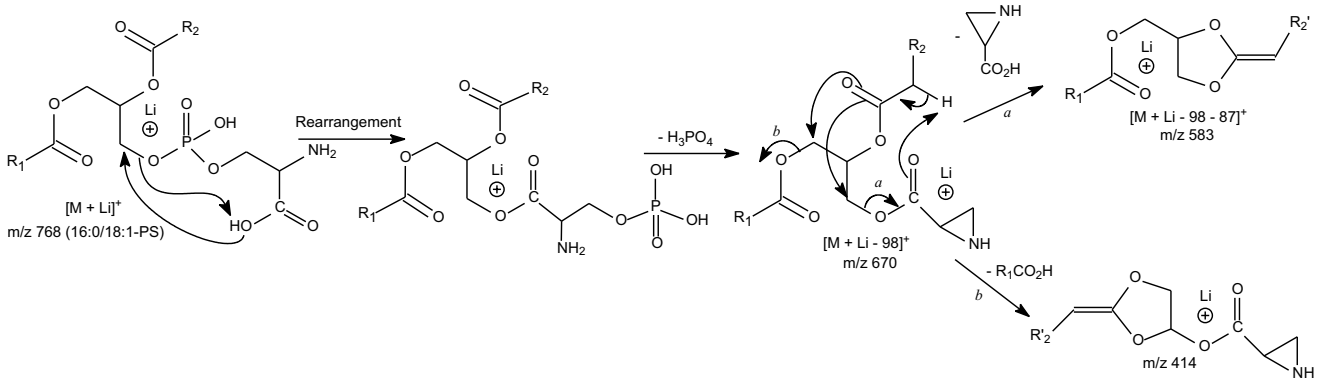

Scheme 4. The fragmentation pathways leading to internal loss of phosphate group proposed for the $[M + Li]^+$ ion of PS. The *m/z* values observed for 16:0/18:1-PS are also shown.

rangement process, which is favored by ITMS but less observable for TSQ because of its multiple collision nature that leads to further fragmentation.

In Figure 4c, the spectrum also contains ions at *m/z* 512 and 486, reflecting losses of the 16:0- and 18:1-acid substituents, respectively, and ions at *m/z* 438 and 412, corresponding to loss of a 1-palmitorylglycerol and of a 2-oleorylglycerol moieties, respectively. These latter two ions are not present in the TSQ product-ion spectrum (Figure 4a), and the origin of these two ions may also involve a rearrangement process followed by loss of an acylglycerol. Again, the features that the *m/z* 512 (768 − R_1CO_2H) ion is more abundant than the *m/z* 486 (768 − R_2CO_2H) ion, and that the *m/z* 438 (768 − $R_1CO_2CH_2CH(OH)CH_2OH$) ion is more abundant than the *m/z* 412 (768 − $HOCH_2CH(OCOR_2)CH_2OH$) ion provide information for assignment of the position of the fatty acyl substituents on the glycerol backbone. Similar results were also observed for the $[M + Li]^+$ ion of 18:0/18:1-PS at *m/z* 796 (Figure 4f).

The product-ion spectrum of the $[M + Na]^+$ ion of 16:0/18:1-PS at *m/z* 784 (Figure 4g) contains ions analogous to those observed in Figure 4a, however, the spectrum is dominated by *m/z* 208, corresponding to a sodiated phosphoserine, and the ion at *m/z* 577 is of low abundance. The results may indicate that cleavage of the C3—OP bond to form the sodiated phosphoserine ion at *m/z* 208 ([phosphoserine + $Na]^+$) becomes more competitive than formation of a protonated $[M + Na - 207]^+$ ion at *m/z* 577, as the Li^+ was replaced by Na^+ (Scheme 4b). This is consistent with the earlier findings that the product-ion spectrum of the $[M + H]^+$ ion of 16:0/18:1-PS is dominated by *m/z* 577 (Scheme 3) and a protonated phosphoserine ion expected at *m/z* 186 is absent (Figure 3a). The IT MS^2-spectrum of the $[M + Na]^+$ ion of 16:0/18:1-PS at *m/z* 784 (Figure 4g) contains ions analogous to those observed in Figure 4c, but the ion at *m/z* 686 from loss of the phosphoric acid moiety declines and the ion at *m/z* 697 reflecting loss of the $C_3H_5NO_2$ moiety becomes the most prominent. Similar results were also observed for the $[M + Na]^+$ ion of 18:0/18:1-PS at *m/z* 812 obtained with a TSQ (Figure 4h) and an IT (Figure 4i) instruments, in which the $[M + Na - 87]^+$ ion at *m/z* 725 is more abundant than *m/z* 714 ($[M + Na - H_3PO_4]^+$). These results also demonstrate that the phosphoric acid moiety is more competitive than its complementary $[M - H_3PO_4]$ moiety for Na^+ to form a sodiated ion, following cleavage of the phosphoric acid moiety. The results are also consistent with the notion that the *m/z* 121 ion ($[H_3PO_4 + Na]^+$) is more abundant than the $[M + Na - H_3PO_4]^+$ ion at *m/z* 686 or at *m/z* 714 in the product-ion spectrum of *m/z* 784 (Figure 4f) or of *m/z* 812 (Figure 4i). In contrast, the analogous ion expected at *m/z* 105 ($[H_3PO_4 + Li]^+$) is nearly absent in the product-ion spectra arising from the $[M + Li]^+$ ion (Figure 4a and b).

The $[M - H + 2Alk]^+$ Ions

The CAD product-ion spectrum of the $[M - H + 2Li]^+$ ion of 16:0/18:1-PS at *m/z* 774 (Figure 5a) is dominated by the *m/z* 687 ion, arising from loss of 87 as described earlier. The cleavage of the C3—OP bond similar to that observed for the $[M + H]^+$ ion (Scheme 3) results in ions at *m/z* 577, reflecting loss of the phosphoserine moiety as a dilithium salt, and at *m/z* 198, corresponding to a dilithiated phosphoserine ion. The ions at *m/z* 431 (687 − 256) and 405 (687 − 282), arise from further losses of the 16:0- and the 18:1-fatty acids from *m/z* 687, respectively. The fact that the *m/z* 431 ion reflecting loss of the fatty acid moiety at *sn*-1 is more abundant than the *m/z* 405 ion reflecting the analogous loss at *sn*-2 provides information for assignment of the position of the fatty acyl substituents. The IT MS^2-spectrum of the $[M - H + 2Li]^+$ ion of 16:0/18:1-PS at *m/z* 774 (Figure 5b) is also dominated by the ion at *m/z* 687 (774 − 87). The consecutive fragmentation process to yield ions at *m/z* 431 and 405 is supported by the IT MS^3-spectrum of the *m/z* 687 ion (774 → 687) (Figure 5c). The $[M - H + 2Li]^+$ ion of 18:0/22:6-PS at *m/z* 848 (Figure 5d) is also dominated by *m/z* 761 and contains major ions at *m/z* 477 (761 − 284) and 433 (61 − 328) from further losses of the 18:0-fatty acyl moiety at *sn*-1 and the 22:6-fatty acyl substituent at *sn*-2, respectively.

The product-ion spectrum of the $[M - H + 2Na]^+$ ion of 16:0/18:1-PS at *m/z* 806 (Figure 5e) obtained with a TSQ instrument contains ions analogous to those observed in Figure 5a, and the spectrum is dominated by the *m/z* 719 (806 − 87) ion. However, the *m/z* 577 ion is less abundant than that observed in Figure 5a, and the ion at *m/z* 230 ($[NaHPO_3OCH_2CH(CO_2)NH_2 + Na]^+$), a sodiated ion of a sodium phosphoserine becomes more abundant than the analogous ion at *m/z* 198 ($[LiHPO_3OCH_2CH(CO_2)NH_2 + Li]^+$) (Figure 5a), which is a lithiated ion of a lithium phosphoserine. Similar results were also observed in the product-ion spectrum of the $[M - H + 2Na]^+$ ion of 18:0/18:1-PS at *m/z* 834 (Figure 5f). The above results are consistent with the notion that cleavage of the C3—OP bond to form the alkali adduct ion of the alkali phosphoserine becomes more competitive than formation of the protonated ion of [M − alkali phosphoserine] moiety as Li^+ was replaced by Na^+, similar to that observed for the $[M + Alk]^+$ ion. The competition between formation of the alkali adduct ion with polar head group and formation of the adduct ion with its complementary moiety becomes so strongly favorable to the former that ions deriving from consecutive fragmentation of the latter ion that leads to structural characterization are lost. This has been observed in the product-ion spectrum of the $[M + Na]^+$ ion as seen earlier.

The $[M - 2H + 3Alk]^+$ Ions

In the presence of alkali metal ions, PS also forms $[M - 2H + 3Alk]^+$ ion by ESI because it contains two acidic

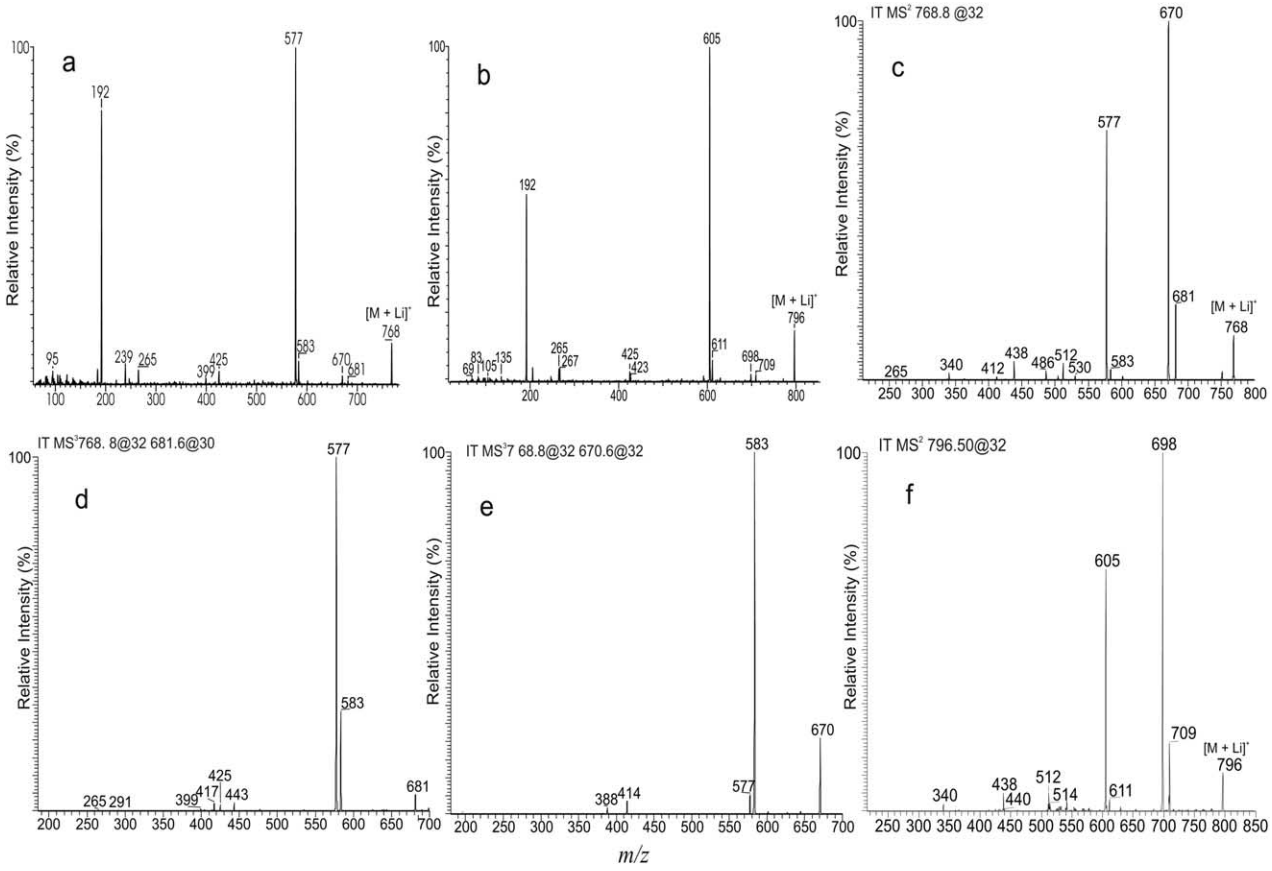

Figure 5. The product-ion spectra of the $[M - H + 2Li]^+$ ion of 16:0/18:1-PS at *m/z* 774 obtained with (**a**) a TSQ instrument and (**b**) an ITMS instrument. (**c**) The IT MS^3-spectrum of the *m/z* 687 ion (774 → 687) arising from *m/z* 774. (**d**)–(**f**) The tandem quadrupole product-ion spectra of (**d**) the $[M - H + 2Li]^+$ ion of 18:0/22:6-PS at *m/z* 848, (**e**) the $[M - H + 2Na]^+$ ion of 16:0/18:1-PS at *m/z* 806, and (**f**) of the $[M - H + 2Na]^+$ ion of 18:0/18:1-PS at *m/z* 834.

protons that can be replaced by alkali metal ions to form an alkali adduct ion of a dialkali salt. Both the MS^2-spectra of the $[M - 2H + 3Na]^+$ ion of 16:0/18:1-PS at *m/z* 828 obtained with a TSQ (Figure 6a) and an ITMS (Figure 6b) instrument are dominated by *m/z* 741 (828 − 87), which is probably equivalent to a sodiated ion of a disodium 16:0/18:1-PA. The ion at *m/z* 572 (828 − R_1CO_2H) arising from loss of 16:0-fatty acid substituent at *sn*-1 is more abundant than *m/z* 546 (828 − R_2CO_2H) arising from loss of the 18:1-fatty acid at *sn*-2. This preferential loss of R_1CO_2H over loss of R_2CO_2H is similar to that observed for phosphatidylcholine (PC), attributable to the fact that the loss of R_1CO_2H probably requires the α-hydrogen of the fatty acyl group at *sn*-2, which is more labile than those at *sn*-1 that participate in the elimination of R_2CO_2H [27].

Further loss of the 18:1- and of the 16:0-fatty acyl substituents as sodium salts from *m/z* 741 gives rise to ions at *m/z* 437 (741 − R_2CO_2Na) and 463 (741 − R_1CO_2Na), respectively. This fragmentation process is supported by the IT MS^3-spectrum of *m/z* 741 (828 → 741) (Figure 6c), which contains major fragment ions similar to those observed in Figure 6a. The *m/z* 437 ion is more abundant than the *m/z* 463 ion in both Figure 6a and c. This is consistent with the notion that loss of the fatty acyl substituents at *sn*-2 is more favorable than the similar loss at *sn*-1. However, ion at *m/z* 485 (741 − R_1CO_2H) arising from loss of the 16:0-fatty acyl substituent at *sn*-1 as an acid is more abundant than the *m/z* 459 ion (741 − R_2CO_2H), arising from loss of the 18:1-acid at *sn*-2. This is also in accord with the conception that loss of the 16:0-acid at *sn*-1 involves the more labile α-hydrogens of the fatty acyl moiety at *sn*-2, while loss of the 18:1-acid involves the less labile α-hydrogens of the fatty acyl moiety at *sn*-1 as described earlier. The observation of a greater abundance of the *m/z* 477 ion (741 − $R'_2CH{=}CO$), arising from loss of the 18:1-fatty acyl ketene at *sn*-2, than the *m/z* 503 ion (741 − $R'_1CH{=}CO$), arising from loss of 16:0-fatty acyl ketene at *sn*-1 is also consistent with the assumption that the α-hydrogens of the fatty acyl moiety at *sn*-2 are more labile than those at *sn*-1 [27].

Ions reflecting the polar head group were observed at *m/z* 252, corresponding to a sodiated disodium salt of phosphoserine and at *m/z* 165, representing a sodiated disodium phosphate ($[Na_2HPO_4 + Na]^+$). The observation of the differential losses of the fatty acyl substituents pertaining to their position on the glycerol back-

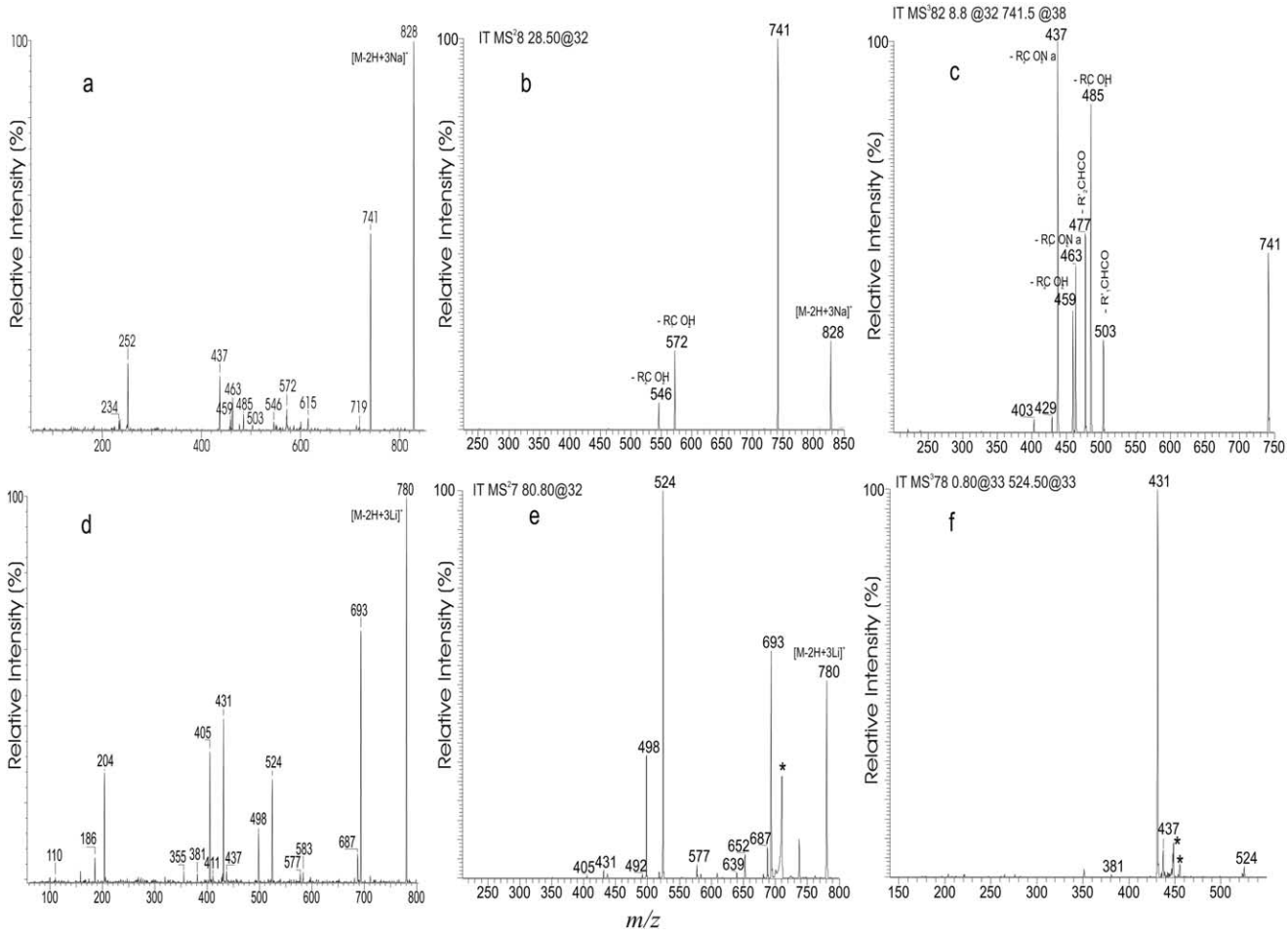

Figure 6. The product-ion spectra of the $[M - 2H + 3Na]^+$ ion of 16:0/18:1-PS at *m/z* 828 obtained with (**a**) a TSQ instrument, (**b**) an ITMS instrument, and (**c**) its IT MS^3-spectrum of the *m/z* 741 ion (828 → 741). (**d**)–(**e**) The product-ion spectra of the $[M - 2H + 3Li]^+$ ion of 16:0/18:1-PS at *m/z* 780 obtained with (**d**) a TSQ instrument, (**e**) an ITMS instrument, and (**f**) its IT MS^3-spectrum of the *m/z* 524 ion (780 → 524).

bone, along with the presence of the ions representing the polar head group permits the structure of PS to be unambiguously unveiled.

The product-ion spectra of the $[M - 2H + 3Li]^+$ ion of 16:0/18:1-PS at *m/z* 780 obtained with a TSQ (Figure 6d) and an ITMS (Figure 6e) instrument contain ions analogous to those observed for the $[M - 2H + 3Na]^+$ ion (Figure 6a and b). However, the ion at *m/z* 431 (693 − $C_{15}H_{31}CO_2Li$) arising from loss of the 16:0-fatty acyl substituent at *sn*-1 as a lithium salt from *m/z* 693 becomes more abundant than *m/z* 405 (693 − $C_{17}H_{33}CO_2Li$), arising from the analogous loss at *sn*-2. This reversal in the abundances of these two ions (compared with the *m/z* 463 and 437 ions in Figure 6a) is attributable to the fact that both the *m/z* 431 and 405 ions arise mainly from *m/z* 524 and 498, respectively, via further loss of the $C_3H_5NO_2$ moiety as a lithium salt (93 Da). These fragmentation pathways are supported by the MS^3-spectra of *m/z* 524 (780 → 524) (Figure 6f) and *m/z* 498 (780 → 498) (not shown). Because the *m/z* 524 ion is preferentially formed over the *m/z* 498 ion in the primary fragmentation process, ion at *m/z* 431 (524 − 93) becomes more abundant than the *m/z* 405 (498 − 93) ion, resulting from consecutive dissociations. The *m/z* 431 and 405 ions can also arise from further decomposition of *m/z* 687, which is equivalent to a lithiated adduct ion of a monolithium salt of 16:0/18:1-PA and undergoes preferential loss of the 16:0-fatty acid to give *m/z* 431 over loss of the 18:1-fatty acid moiety to give *m/z* 405. This fragmentation process has been described for the $[M - H + 2Li]^+$ ion of 16:0/18:1-PS at *m/z* 774 (Figure 5a and c). The consecutive fragmentation of the *m/z* 693 ion (780 → 693) (not shown) also yields ions at *m/z* 431 and 405 but requires higher collision energy than do the *m/z* 524 and 498 ions that yield the similar ions, and thus the pathway is less favorable. As a result, the *m/z* 431 ion is more prominent than *m/z* 405 in the product-ion spectrum observed for the $[M - 2H + 3Li]^+$ ion of 16:0/18:1-PS.

Conclusions

The tandem mass spectrometry of the various molecular ions of phosphatidylserine generated by ESI as described above represents the broad applicability of various molecular ions of phospholipids that can be

exploited for structural characterization. The tandem mass spectrum of the $[M - H]^-$ ion of PS contains complete structural information and offers the utmost sensitivity for structural determination. In contrast, product-ion spectra from the $[M + H]^+$ species are rather simple and are less useful for structural characterization. The product-ion spectra arising from $[M - 2H + Alk]^-$, $[M + Alk]^+$, $[M - H + 2Alk]^+$, and $[M - 2H + 3Alk]^+$ (where Alk = Li, Na), on the other hand, contain multiple sets of fragment ions informative for identification of the polar head group, the fatty acyl substituents, and their positions on the glycerol backbone. The rearrangement process leading to internal loss of the phosphate moiety observed in the IT MS^2-spectra of the $[M + Alk]^+$ ions of PS is unique. Another interesting note from this study is that the IT MS^2-spectrum of the $[M - 2H + 3Li]^+$ ion at *m/z* 780 (Figure 6c) along with its IT MS^3-spectra of the *m/z* 524 (780 → 524, Figure 6f) and *m/z* 693 ions (780 → 693, not shown), as well as the IT MS^3-spectrum of the *m/z* 687 ion (774 → 687, Figure 5c) from the $[M - H + 2Li]^+$ ion at *m/z* 774 also contain several ions that are broad and asymmetric (marked with an asterisk). In contrast, the analogous ions are not present in the spectra arising from the corresponding $[M - 2H + 3 Na]^+$ (Figure 6b and c) and $[M - H + 2Na]^+$ (806 → 719, not shown) species. Asymmetric peaks resulting from peak fronting observed by ITMS have been previously reported and were thought to arise from "fragile" precursors during application of resonance ejection in mass analysis [30, 31]. The mechanisms leading to the rearrangement process as well as to the formation of the asymmetric ions as observed in this study are currently under investigation.

Acknowledgments

This research was supported by U.S. Public Health Service grants P41-RR-00,954, R37-DK-34,388, P60-DK-20,579, P01-HL-57,278, P30-DK-56,341, and a grant (996003) from the Juvenile Diabetes Foundation. The authors thank the reviewers for their critical comments on this manuscript.

References

1. Folch, J. The chemical structure of phosphatidylserine. *J. Biol. Chem.* **1948,***17,* 439–450.
2. Baer, E.; Maurukas, J. Phosphatidylserine. *J. Biol. Chem.* **1955,** *212,* 25–38.
3. Baer, E.; Maurukas, J. The diazomethol ysis of glycerolphosphatides: A novel method of determining the configuration of phosphatidylserines and cephalins. *J. Biol. Chem.* **1955,** *212,* 39–48.
4. Kanfer, J.; Kennedy, E. P. Metabolism and function of bacterial lipids: II. Biosynthesis of phospholipids in *Escherichia coli*. *J. Biol. Chem.* **1964,** *239,* 1720–1726.
5. Hübscher, H. G.; Dils, R. R.; Pover, W. F. R. Studies on the biosynthesis of phosphatidylserine. *Biochim. Biophys. Acta* **1959,** *36,* 518–528.
6. Dennis, E. A.; Kennedy, E. P. Enzymatic synthesis and decarboxylation of phosphatidylserine in *Tetrahymena pyriformis*. *J. Lipid Res.* **1970,** *11,* 394–403.
7. Bittova, L.; Stahelin, R. V.; Cho, W. Roles of ionic residues of the C1 domain in protein kinase C-A activation and the origin of phosphatidylserine specificity. *J. Biol. Chem.* **2001,** *276,* 4218–4226.
8. Stekhoven, F. M.; Tijmes, J.; Umeda, M.; Inoue, K.; De Pont, J. J. Monoclonal antibody to phosphatidylserine inhibits Na+/K(+)-ATPase activity. *Biochim. Biophys. Acta* **1994,** *1194,* 155–165.
9. Hofmann, K.; Tomiuk, S.; Wolff, G.; Stoffel, W. Cloning and characterization of the mammalian brain-specific, Mg^{2+}-dependent neutral sphingomyelinase. *Proc. Natl. Acad. Sci. U.S.A.* **2000,** *97,* 5895–5900.
10. Tamiya-Koizumi, K.; Kojima, K. Activation of magnesium-dependent, neutral sphingomyelinase by phosphatidylserine. *J. Biochem.* (Tokyo) **1986,** *99,* 1803–1806.
11. Bevers, E.; Comfurius, P.; van Rijn, J.; Hemker, H.; Zwaal, R. Generation of prothrombin-converting activity and the exposure of phosphatidylserine at the outer surface of platelets. *Eur. J. Biochem.* **1982,** *122,* 429–436.
12. van den Eijnde, S. M.; van den Hoff, M. J. B.; Reutelingsperger, C. P. M.; van Heerde, W. L.; Henfling, M. E. R.; Vermeij-Keers, C.; Schutte, B.; Borgers, M.; Ramaekers, F. C. S. Transient expression of phosphatidylserine at cell-cell contact areas is required for myotube formation. *J. Cell Sci.* **2001,** *114,* 3631–3642.
13. Fadok, V. A.; Voelker, D. R.; Campbell, P. A.; Cohen, J. J.; Bratton, D. L.; Henson, P. M. Exposure of phosphatidylserine on the surface of apoptotic lymphocytes triggers specific recognition and removal by macrophages. *J. Immunol.* **1992,** *148,* 2207–2216.
14. Fadok, V. A.; de Cathelineau, A.; Daleke, D. L.; Henson, P. M.; Bratton, D. L. Loss of phospholipid asymmetry and surface exposure of phosphatidylserine is required for phagocytosis of apoptotic cells by macrophages and fibroblasts. *J. Biol. Chem.* **2001,** *276,* 1071–1077.
15. Bennett, M. R.; Gibson, D. F.; Schwartz, S. M.; Tait, J. F. Binding and phagocytosis of apoptotic vascular smooth muscle cells is mediated in part by exposure of phosphatidylserine. *Circ. Res.* **1995,** *77,* 1136–1142.
16. Martin, S. J.; Reutelingsperger, C. P.; McGahon, A. J.; Rader, J. A.; van Schie, R. C.; LaFace, D. M.; Green, D. R. Early redistribution of plasma membrane phosphatidylserine is a general feature of apoptosis regardless of the initiating stimulus: Inhibition by overexpression of Bcl-2 and Abl. *J. Exp. Med.* **1995,** *182,* 1545–1556.
17. Schlegel, R. A.; Callahan, M. K.; Williamson, P. The central role of phosphatidylserine in the phagocytosis of apoptotic thymocytes. *Annals N.Y. Acad. Sci.* **2000,** *926,* 217–225.
18. Tyurina, Y. Y.; Shvedova, A. A.; Kawai, K.; Tyurin, V. A.; Kommineni, C.; Quinn, P. J.; Schor, N. F.; Fabisiak, J. P.; Kagan, V. E. Phospholipid signaling in apoptosis: Peroxidation and externalization of phosphatidylserine. *Toxicology* **2000,** *148* (2/3), 93–101.
19. Li, M. O.; Sarkisian, M. R.; Mehal, M. Z.; Rakic, P.; Flavell, R. A. Phosphatidylserine receptor is required for clearance of apoptotic cells. *Science* **2003,** *302* (5650), 1560–1563.
20. Chen, S.; Kirschner, G.; Traldi, P. Positive ion fast atom bombardment mass spectrometric analysis of the molecular species of glycerophosphatidylserine. *Anal. Biochem.* **1990,** *191,* 100–105.
21. Murphy, R. C.; Harrison, K. A. Fast atom bombardment mass spectrometry of phospholipids. *Mass Spectrom. Rev.* **1994,** *13,* 57–75.

22. Ho, Y. P.; Huang, P. C.; Deng, K. H. Metal ion complexes in the structural analysis of phospholipids by electrospray ionization tandem mass spectrometry. *Rapid Commun. Mass Spectrom.* **2003,** *17,* 114–21.
23. Pulfer, M.; Murphy, R. C. Electrospray mass spectrometry of phospholipids. *Mass Spectrom. Rev.* **2003,** *22,* 332–364.
24. Hsu, F.-F.; Turk, J. Charge-driven fragmentation processes in diacyl glycerophosphatidic acids upon low-energy collisional activation. A mechanistic proposal. *J. Am. Soc. Mass Spectrom.* **2000,** *11,* 797–803.
25. Hsu, F-F.; Turk, J. Charge-driven and charge-remote fragmentation processes in diacyl glycerophosphoethanolamine upon low-energy collisional activation. A mechanistic proposal. *J. Am. Soc. Mass Spectrom.* **2000,** *11,* 892–899.
26. Hsu, F.-F.; Turk, J. Characterization of phosphatidylethanolamine as a lithiated adduct by triple quadrupole tandem mass spectrometry with electrospray ionization. *J. Mass. Spectrom.* **2000,** *35,* 595–606.
27. Hsu, F.-F.; Turk, J. Electrospray ionization/tandem quadrupole mass spectrometric studies on phosphatidylcholines: The fragmentation processes. *J. Am. Soc. Mass Spectrom.* **2003,** *14,* 352–363.
28. Hsu, F.-F.; Turk, J. Structural characterization of triacylglycerols as lithiated adducts by electrospray ionization mass spectrometry using low-energy collisionally activated dissociation on a triple stage quadrupole instrument. *J. Am. Soc. Mass Spectrom.* **1999,** *10,* 587–599.
29. Hsu, F.-F.; Bohrer A.; Turk, J. Formation of lithiated adducts of glycerophosphocholine lipids facilitates their identification by electrospray ionization tandem mass spectrometry. *J. Am. Soc. Mass Spectrom.* **1998,** *9,* 516–526.
30. McClellan, J. E.; Murphy, J. P., III; Mulholland, J. J.; Yost, R. A. Effect of fragile ions on mass resolution and on isolation for tandem mass spectrometry in the quadrupole ion trap mass spectrometer. *Anal. Chem.* **2002,** *74,* 402–412.
31. Murphy, J. P., III; Yost, R. A. Origin of mass shifts in the quadrupole ion trap: Dissociation of fragile ions observed with a hybrid ion trap/mass filter instrument. *Rapid Commun. Mass Spectrom.* **2000,** *14,* 270–273.